# Nanoporous gold plasmonic structures for sensing applications

**G. Ruffato,[1,2,3,*] F. Romanato,[1,2,3] D. Garoli,[1,2,3] and S. Cattarin[4]**

[1]*Department of Physics "G. Galilei," University of Padova, via Marzolo 8, 35131 Padova, Italy*
[2]*LaNN Laboratory for Nanofabrication of Nanodevices, VenetoNanotech, Corso Stati Uniti 4, 35127 Padova, Italy*
[3]*Institute for Materials Manufacturing (IOM-CNR), Area-Science Park, Basovizza 34012, Trieste, Italy*
[4]*Institute for Energetics and Interphases (IENI-CNR), Corso Stati Uniti 4, 35127 Padova, Italy*
**gianluca.ruffato@unipd.it*

**Abstract:** The fabrication, characterization and functionalization of periodically patterned nanoporous gold layers is presented. The material shows plasmonic properties in the near infrared range, with excitation and propagation of surface plasmon polaritons. Functionalization shows a marked enhancement in the optical response in comparison with evaporated gold gratings, due to a great increase of the active surface. Due to its superior response, nanoporous gold patterns appear promising for the realization of compact plasmonic platforms for sensing purposes.



**OCIS codes:** (240.6680) Surface plasmons; (160.4236) Nanomaterials; (280.4788) Optical sensing and sensors.

## References and links

1. S. A. Maier, ed., *Plasmonics— Fundamentals and Applications* (Springer, 2007).
2. J. Homola, "Surface plasmon resonance sensors for detection of chemical and biological species," Chem. Rev. **108**(2), 462–493 (2008).
3. J. Biener, G. W. Nyce, A. M. Hodge, M. M. Biener, A. V. Hamza, and S. A. Maier, "Nanoporous plasmonic metamaterials," Adv. Mater. (Deerfield Beach Fla.) **20**(6), 1211–1217 (2008).
4. N. A. Senior and R. C. Newman, "Synthesis of tough nanoporous metals by controlled electrolytic dealloying," Nanotechnology **17**(9), 2311–2316 (2006).
5. T. Fujita, L. H. Qian, K. Inoke, J. Erlebacher, and M. W. Chen, "Three-dimensional morphology of nanoporous gold," Appl. Phys. Lett. **92**(25), 251902 (2008).
6. X. Lu, E. Bischoff, R. Spolenak, and T. J. Balk, "Investigation of dealloying in Au-Ag thin films by quantitative electron probe microanalysis," Scr. Mater. **56**(7), 557–560 (2007).
7. X. Y. Lang, P. F. Guan, L. Zhang, T. Fujita, and M. W. Chen, "Characteristic length and temperature dependence of surface enhanced Raman scattering of nanoporous gold," J. Phys. Chem. C **113**(25), 10956–10961 (2009).
8. E. Detsi, M. van de Schootbrugge, S. Punzhin, P. R. Onck, and J. T. M. De Hosson, "On tuning the morphology of nanoporous gold," Scr. Mater. **64**(4), 319–322 (2011).
9. A. I. Maaroof, A. Gentle, G. B. Smith, and M. B. Cortie, "Bulk and surface plasmons in highly nanoporous gold films," J. Phys. D Appl. Phys. **40**(18), 5675–5682 (2007).
10. F. Yu, S. Ahl, A. M. Caminade, J. P. Majoral, W. Knoll, and J. Erlebacher, "Simultaneous excitation of propagating and localized surface plasmon resonance in nanoporous gold membranes," Anal. Chem. **78**(20), 7346–7350 (2006).
11. F. Romanato, H. K. Kang, K. H. Lee, G. Ruffato, M. Prasciolu, and C. C. Wong, "Interferential lithography of 1D thin metallic sinusoidal grtings: accurate control of the profile for azimuthal angular dependent plasmonic effects and applications," Microelectron. Eng. **86**(4-6), 573–576 (2009).
12. F. Romanato, K. H. Lee, H. K. Kang, G. Ruffato, and C. C. Wong, "Sensitivity enhancement in grating coupled surface plasmon resonance by azimuthal control," Opt. Express **17**(14), 12145–12154 (2009).
13. F. Romanato, K. H. Lee, G. Ruffato, and C. C. Wong, "The role of polarization on surface plasmon polariton excitation on metallic gratings in the conical mounting," Appl. Phys. Lett. **96**(11), 111103 (2010).
14. Y. Sun and T. J. Balk, "Evolution of structure, composition, and stress in nanoporous gold thin films with grain-boundary cracks," Metall. Mater. Trans., A Phys. Metall. Mater. Sci. **39**(11), 2656–2665 (2008).
15. S. Cattarin, D. Kramer, A. Lui, and M. Musiani, "Preparation and characterization of gold nanostructures of controlled dimension by electrochemical techniques," J. Phys. Chem. C **111**(34), 12643–12649 (2007).
16. S. Cattarin, D. Kramer, A. Lui, and M. Musiani, "Formation of nanostructured gold sponges by anodic dealloying: EIS investigation of product and process," Fuel Cells (Weinh.) **9**(3), 209–214 (2009).
17. R. L. Aggarwal, L. W. Farrar, E. D. Diebold, and D. L. Polla, "Measurement of the absolute Raman scattering cross section of the 1584-$cm^{-1}$ band of benzenethiol and the surface-enhanced Raman scattering cross section

#146763 - $15.00 USD Received 29 Apr 2011; revised 1 Jun 2011; accepted 1 Jun 2011; published 22 Jun 2011

enhancement factor for femtosecond laser-nanostructured substrates," J. Raman Spectrosc. **40**(9), 1331–1333 (2009).
18. E. D. Palik, ed., *Handbook of Optical Constants of Solids* (Academic Press, 1991).
19. M. C. Dixon, T. A. Daniel, M. Hieda, D. M. Smilgies, M. H. W. Chan, and D. L. Allara, "Preparation, structure, and optical properties of nanoporous gold thin films," Langmuir **23**(5), 2414–2422 (2007).
20. N. W. Ashcroft and N. D. Mermin, eds., *Solid State Physics* (Thomson Brookes – Cole, 1976).

## 1. Introduction

In the recent decades Plasmonics has known an increasing employment in the research and realization of sensing devices for gas detection and liquid analysis [1,2]. Surface plasmon polaritons (SPPs) are evanescent electromagnetic waves bound to metal-dielectric interfaces that arise from the coupling of EM-fields with conduction electron oscillations inside the metal [1]. The high localization makes SPPs extremely sensitive to local refractive index changes on the surface and therefore SPPs represent a powerful instrument for label-free sensing purposes [2]. Research is driven by the desire to create materials with designed photonic properties taking advantage of electromagnetic resonances and concomitant enhancement of the electromagnetic near-field owing to surface plasmons. In the continuous search for new materials capable of better performances Nanoporous Gold (NPG) offers an extensive surface where the analytes can bind and thereby an increased sensitivity and efficiency [3].

NPG may be formed by a spontaneous pattern-forming instability during the chemical etching of silver from gold-silver alloys [4]. The leaching of the less noble metal gives rise to a bicontinuous sponge-like structure of nanopores and gold ligaments [5] whose geometric features depend on the alloy composition and on the experimental conditions of the dealloying process [4–8]. The nanoporous structure affects also the optical properties: the plasma frequency $\omega_p$ exhibits red-shift due to the lower density in comparison with bulk gold and the material shows metallic behaviour for wavelengths above the near-IR range [9].

Application of NPG in Kretschmann's configuration has been previously reported by Yu et al. [10]. They demonstrated excitation of propagating surface plasmon resonances on nanoporous gold membranes in a multilayer system under condition of total internal reflection of the probe light source. The aim of this work is to design and fabricate a SPP-supporting substrate that exploits NPG properties and that avoids the cumbersome prism presence and the related alignment problems. For the first time so far as we know, NPG surface has been periodically patterned in order to exploit grating coupling so to excite propagating surface plasmons. Because of red-shift of plasmonic properties, grating period and amplitude have to be properly designed to give rise to SPP resonances in the near-IR region. The alignment of the plasmonic grating has been performed in conical configuration exploiting the degree of freedom of azimuthal rotation and polarization in order to optimize the sensitivity [11–13]. The result is a conductive metallic material with a greatly enhanced surface to volume ratio which is particularly suitable for the realization of plasmonic supports for sensing purposes.

## 2. Experimental

A 240 nm thick $Ag_{75}Au_{25}$ alloy layer was deposited over a 100 nm layer of pure gold which was in turn deposited over a 5 nm intra-layer of Cr that improves the adhesion to the glass substrate [14]. The alloy deposition experiments were performed by means of a DC turbo sputter coater (Emitech K575X, Emitech Ltd., Ashford, Kent, UK). The silver/gold alloy was sputtered at room temperature from a ($Ag_{62.3}/Au_{37.7}$ wt%, GoodFellow) sputtering target in an Ar gas atmosphere at a pressure of $7 \cdot 10^{-3}$ mbar. The dealloying process has been performed electrochemically, by anodic treatment in 0.1 M $HClO_4$ at 65°C, for 30 min, at the constant applied potential E = 0.98 V vs SCE (saturated calomel electrode), in analogy to a procedure already discussed in previous papers [15,16]. To ensure elimination of possible salt residues the samples were then washed in two steps, first in a fresh 0.1 M HClO4 solution (1 h), then in distilled water (2 times, 1 h each), gently dried in a nitrogen stream and stored. The anodic

#146763 - $15.00 USD Received 29 Apr 2011; revised 1 Jun 2011; accepted 1 Jun 2011; published 22 Jun 2011

treatment causes Ag leaching and leaves a porous Au layer (with some residual Ag). The roughness factor $f_r = SA/A$, defined as the ratio between a measured effective surface area *SA* and the corresponding geometric area *A*, has been estimated by electrochemical impedance spectroscopy (EIS) [15,16], which allows measurement of the interface capacity - a quantity proportional to the effective surface area - on porous and smooth flat electrodes. Experimental $f_r$ values were typically in the range 12-14 for the 240 nm thick NPG layer.

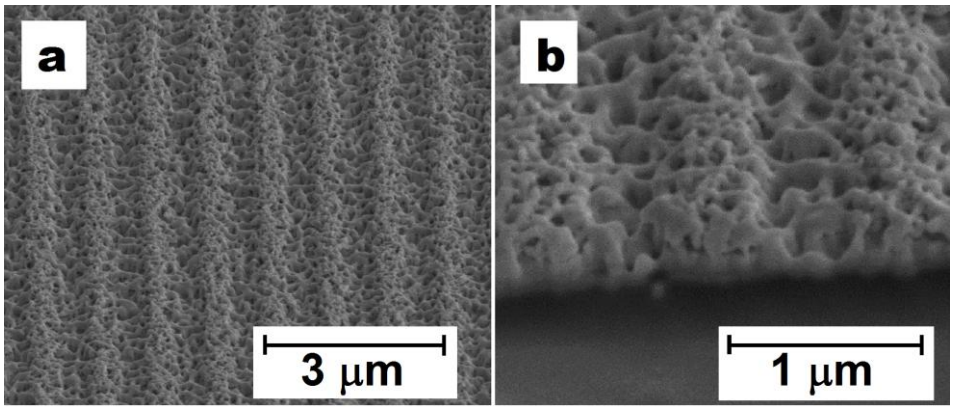


Fig. 1. SEM micrographs of the FIB pattern on the nanoporous gold surface (a) and cross-section (b).

Nanoporous gold optical response was measured with a J. A. Woollam Co. VASE ellipsometer with angular and wavelength spectroscopic resolution of 0.005° and 0.3 nm respectively. Spectroscopic Ellipsometry with rotating polarizer analysis was recorded in the wavelength range between 300 and 2400 nm (10 nm step) at three different angles of incidence (50°, 60°, 70°) on the no-patterned area of NPG sample. Focused Ion Beam (FIB) lithography was performed by means of the ion source of the dual beam system using 30 kV of accelerating voltage and a beam probe current of 280 pA. Taking into account the lower plasma frequency of NPG and the resulting shift of metallic behavior in the IR range (see section 3 "Results and Discussion"), a grating about 50 nm thick with a period of 1000 nm (duty cycle 0.5) has been patterned (Fig. 1(a)) over an area 640 μm x 640 μm. A cross section of the grating pattern shows that the typical amplitude of the grating is confined within the first 70 nm of the surface NPG (Fig. 1(b)). For comparison with the gold NPG case, a grating with period of about 400 nm was patterned on a typical gold bulk film of 80 nm thickness evaporated over a silicon substrate.

A self-assembled monolayer (SAM) of benzenethiol (Thiophenol, $C_6H_5SH$) was deposited on the gold coated grating surfaces at room temperature. The substrates were submerged in a 3-mM solution of benzenethiol in methanol for about 48 hrs, then rinsed thoroughly with ethanol for at least 5 minutes and dried in a nitrogen stream [17]. Measurements on gold gratings were performed in air environment in a θ/2θ symmetric reflectivity configuration, with θ scanned with step size of 0.2°, using ellipsometer 75 W Xe lamp, monochromatized at $\lambda = 1400$ nm for NPG grating and at $\lambda = 600$ nm for the evaporated gold (EVG) grating.

## 3. Results and discussion

In Fig. 2 experimental optical constants of NPG are compared with those of bulk gold [18]. It appears a weaker metallic behaviour in the optical regime with $\varepsilon_1$ nearly close to zero. Above the 900 nm, $\varepsilon_2$ of NPG is smaller than for the bulk case and $\varepsilon_1$ starts to be sufficiently negative to show a metallic behaviour.

#146763 - $15.00 USD Received 29 Apr 2011; revised 1 Jun 2011; accepted 1 Jun 2011; published 22 Jun 2011

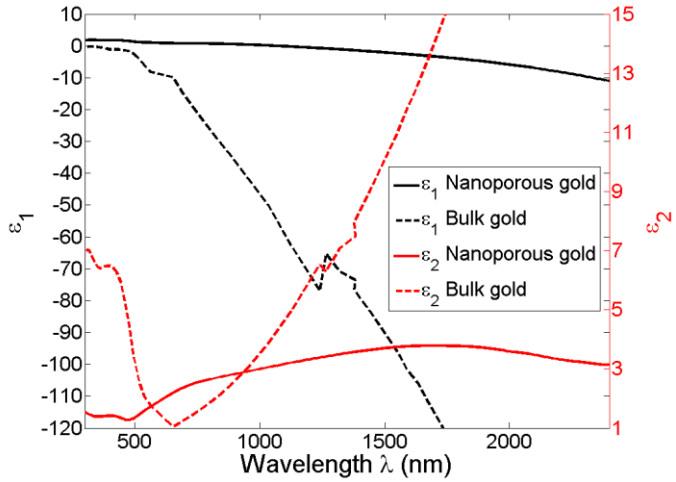


Fig. 2. Dielectric permittivity of nanoporous gold. Comparison with tabulated buk gold values.

The behavior of the dielectric constants must be considered when a grating is designed in order to support propagating plasmonic modes. The geometry of the grating (duty cycle, period and thickness of the walls) was fixed in order to obtain a plasmonic resonance in the spectral range in which the material exhibits a metallic behavior. To understand the optical response, we examine the effective frequency-dependent dielectric function ε(ω) and describe it with a Lorentz-Drude model in the UV-VIS-nearIR range:

$$\varepsilon(\omega) = \varepsilon_\infty + \varepsilon_{UV}(\omega) + \varepsilon_D(\omega) + \varepsilon_{IR}(\omega)$$
$$= \varepsilon_\infty - \frac{A_{UV}}{\omega^2 - \omega_{UV}^2 + i\omega\omega_{\tau,UV}} - \frac{\omega_p^2}{\omega^2 + i\omega\omega_{\tau,D}} - \frac{A_{IR}}{\omega^2 - \omega_{IR}^2 + i\omega\omega_{\tau,IR}} \quad (1)$$

where $\varepsilon_\infty$ takes into account the constant contribution to polarization due to *d* band electrons close to the Fermi surface. $\varepsilon_{UV}(\omega)$ is a Lorentz oscillator that describes the *3d* energy band-to-Fermi Level interband transition centered at a frequency $\omega_{UV}$ in the UV range with a band-width $\omega_{\tau,UV}$. The term $\varepsilon_D(\omega)$ represents the Drude contribution due to free *s*-electrons. The Lorentz contribution $\varepsilon_{IR}(\omega)$ considered in order to model the behavior of the dielectric response in the near IR range, enables excellent fits to dielectric constant of nanoporous films [9] and it is probably associated to the excitation of Localized Surface Plasmons.

Permittivity values calculated from ellipsometric analysis have been fitted with the oscillator model both for NPG and EVG in order to get an estimation of the fitting parameters (Table 1). In NPG the intraband absorption amplitude $A_{UV}$ is lower than in EVG. This is explained by the fact that inside gold ligaments each Au atom interacts with much fewer atoms than in bulk metal and results in a discretization of dipole transition between *sp* electron eigenstates and in the weakening or disappearance of the transition of *d* electrons to conduction band [19]. The reorganization of gold atoms also affects the relaxation time $\tau$ of free carriers in the Drude term which is shorter for NPG ($\tau_{NPG}$ = 3.5 fs) than for EVG ($\tau_{EVG}$ = 10.1 fs), since it is related to the scattering processes in the material. The plasma frequency $\omega_{p,NPG} = 3.4 \cdot 10^3$ THz (2.26 eV) is lower than for bulk gold ($\omega_{p,EVG} = 12.7 \cdot 10^3$ THz, 8.36 eV) and metallic behaviour is shifted towards greater wavelengths in the near-IR region. This optical property, originated from the nanoscale morphology, is the main responsible of the copper-bronze colour, much darker than the typical yellowish bright colour of compact gold. The density *N* of free carrier can be estimated from plasma frequency $\omega_p$ [20]:

#146763 - $15.00 USD Received 29 Apr 2011; revised 1 Jun 2011; accepted 1 Jun 2011; published 22 Jun 2011

$$N = \frac{m\varepsilon_0\omega_p^2}{e^2} \tag{2}$$

where $e$ and $m$ are electron charge and mass and $\varepsilon_0$ is the void permittivity. As expected, free-electron density in nanoporous gold $N_{NPG} = 3.70 \cdot 10^{21}$ cm$^{-3}$ is much lower than in bulk gold $N_{EVG} = 5.08 \cdot 10^{22}$ cm$^{-3}$.

**Table 1. Parameters of Eq. (1) from the Fit of Permittivity Experimental Data for Nanoporous Gold (NPG) and Evaporated Gold (EVG)**

| | $\varepsilon_\infty$ | $\omega_p$ (eV) | $\omega_\tau$ (eV) | $A_{UV}$ (eV$^2$) | $\omega_{UV}$ (eV) | $\omega_{\tau,UV}$ (eV) | $A_{IR}$ (eV$^2$) | $\omega_{IR}$ (eV) | $\omega_{\tau,IR}$ (eV) |
|---|---|---|---|---|---|---|---|---|---|
| *NPG* | 1.63 | 2.26 | 1.20 | 28.5 | 5.11 | 3.82 | 6.73 | 1.55 | 2.06 |
| *EVG* | 5.92 | 8.36 | 0.41 | 86.6 | 4.71 | 3.15 | - | - | - |

Reflectivity analysis after FIB lithography shows the appearance of resonance dips in the *near*-IR in correspondence of the excitation of propagating surface plasmons on the porous gold surface (Fig. 3). The excitation of SPPs on a grating is achieved when the on-plane component of the incident light wave-vector and the diffracted SPP wave-vector $\vec{k}_{SPP}$ match the momentum conservation condition:

$$\vec{k}_{SPP} = \vec{k}_{in_\parallel} \pm n\vec{G} \tag{3}$$

where $\vec{k}_{in_\parallel} = \frac{2\pi}{\lambda}(\sin\theta_{in}, 0)$ and $\theta_{in}$ is the angle of incidence. The crystal momentum of the grating of $\Lambda$ pitch is $\vec{G} = \frac{2\pi}{\Lambda}(\cos\phi, \sin\phi)$ whose rotation is measured by $\phi$ (see inset picture in Fig. 4). Only the first diffraction order (n = 1) is effective because in our case, $G$ is always greater than $k_{in\ ||}$. Dip features such as width, depth and position strictly depend on the properties of the supporting material, i.e. optical constants of the nanoporous gold layer.

Reflectivity data for increasing azimuth angles have been collected before and after functionalization of gold surfaces with benezenethiol. In a previous work we demonstrated how the azimuthal rotation of the grating can enhance sensing capability up to at least one order of magnitude [12]. Furthermore, after grating azimuthal rotation, *p*-Polarization is no longer the most effective for SPP excitation and incident polarization must be tuned to the optimal value in order to enforce coupling strength and optimize resonance depth [13]. Data points in Fig. 4 show the increase of resonance angle shift with azimuth rotation for the optimized polarization α of light (α = 0° for p-polarization, i.e. the electric field lies on the scattering plane). At the limit azimuth value of 45° and polarization α = 140°, a shift $\Delta\theta_{NPG}(45°) = 4.05°$ is measured, which is almost 65 times grater than the shift for null azimuth and *p*-polarization $\Delta\theta_{NPG}(0°) = 0.06°$ (α = 0°). Resonance dips become broader for increasing azimuth value, however the resonance angle shift Δθ scales with a factor greater than the enlargement of the dip full width half maximum $\Delta\theta_{FWHM}$. Thus the angular figure of merit $FOM_\theta = \Delta\theta/\Delta\theta_{FWHM}$ increases and the detection improvement by azimuthal rotation is preserved [12]. In our case $FOM_\theta(\phi = 45°) = 0.277$ that is 18.5 times greater than $FOM_\theta(0°) = 0.015$.

#146763 - $15.00 USD Received 29 Apr 2011; revised 1 Jun 2011; accepted 1 Jun 2011; published 22 Jun 2011

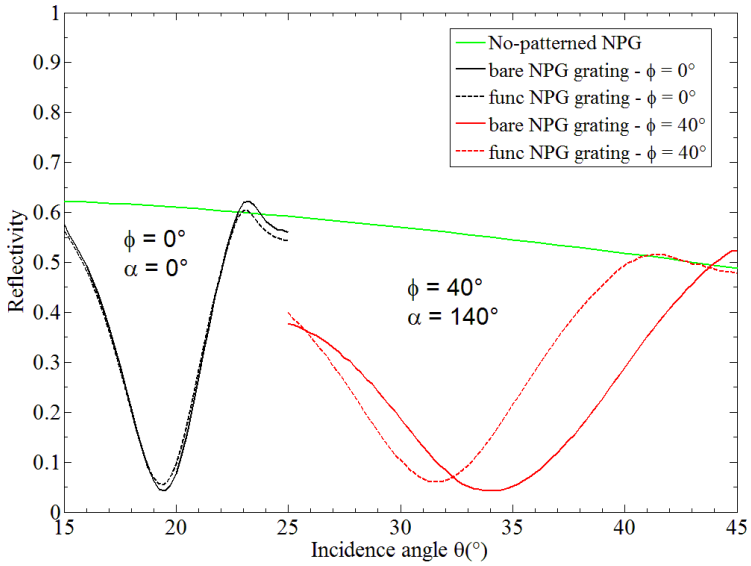


Fig. 3. Reflectivity measurements for NPG grating before (solid line) and after (dashed line) functionalization at null azimuth (black line) and p-polarization ($\alpha = 0°$), and at azimuth 40° (red line), polarization $\alpha = 140°$. Green solid line: reflectivity data for no-patterned NPG surface.

In order to compare the sensitivity of the plasmonic gratings, reflectivity data have been also compared with the optical response of an evaporated gold (EVG) grating after the same functionalization process. EVG surface has been patterned with a period $\Lambda = 400$ nm in order to excite SPPs in the visible range, where the angular response for EVG is greater since the sensitivity to a thin coating layer decreases with wavelength [2]. For incident $\lambda = 600$ nm and azimuth $\phi = 45°$ ($\alpha = 135°$) we measure a shift $\Delta\theta_{EVG}(45°) = 0.82°$.

The choice of evaluating the EVG and NPG gratings at different wavelength has been motivated to compare them at the respective maximum of sensibility. The greater dip shift in the case of patterned NPG is explained by the enhanced binding surface per unit area of the nanopores. Analyte molecules in fact, not merely bind in the form of a thin coating layer on the outer surface, but, in the case of NPG, penetrate into the pores and bind to the inner surface, inducing a greater change of the effective index of the plasmonic support.

#146763 - $15.00 USD Received 29 Apr 2011; revised 1 Jun 2011; accepted 1 Jun 2011; published 22 Jun 2011

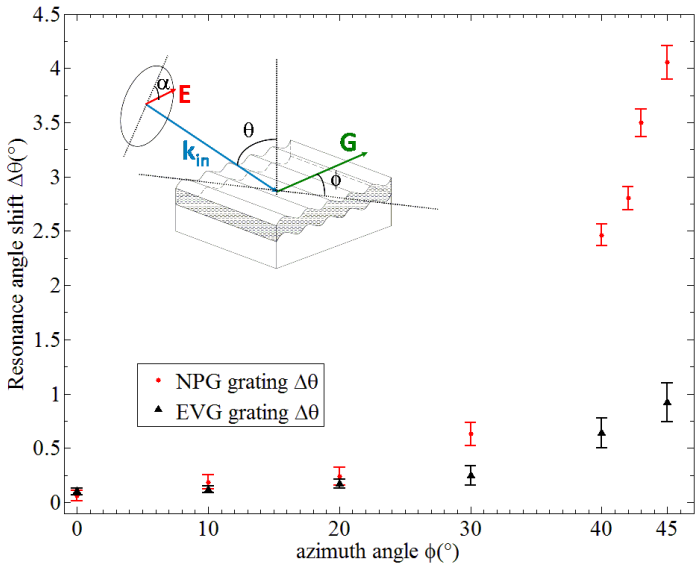


Fig. 4. Resonance angle shift Δθ as a function of azimuth rotation after functionalization with a benzenethiol self-assembled monolayer. Experimental data of functionalized nanoporous gold (NPG) grating (period Λ = 1000 nm, incident wavelength λ = 1400 nm – red points) are compared with experimental shifts for an evaporated-gold (EVG) grating (Λ = 400 nm, λ = 600 nm – black points). Inset picture: scheme of the incidence mounting.

## 4. Conclusions

In summary, we presented our work of fabrication, characterization and design of periodically patterned nanoporous gold surfaces that support excitation of propagating surface plasmons. Thanks to a greatly enhanced surface-to-volume ratio, nanoporous gold reveals benefits for better reaction efficiency and detection sensitivity. Functionalization shows an enhancement in the optical response in comparison with evaporated gold gratings. Thus nanoporous gold represents a useful and promising material for the realization of compact sensitive devices based on SPP plasmonic substrate for sensing purposes in a large variety of fields: environmental protection, biotechnology, medical diagnostics, drug screening, food safety and security.

## Acknowledgments

This work has been supported by a grant from “Fondazione Cariparo” – Surface PLasmonics for Enhanced Nano Detectors and Innovative Devices (SPLENDID) – Progetto Eccellenza 2008 and from University of Padova – Progetto di Eccellenza “Platform”.

#146763 - $15.00 USD Received 29 Apr 2011; revised 1 Jun 2011; accepted 1 Jun 2011; published 22 Jun 2011